Molecular Pharmacology Fast Forward. Published on December 21, 2017 as DOI: 10.1124/mol.117.109827
This article has not been copyedited and formatted. The final version may differ from this version.

MOL #109827

Title:

(*Z*)-2-(3,4-Dichlorophenyl)-3-(1*H*-pyrrol-2-yl)acrylonitrile exhibits selective anti-tumour activity in breast cancer cell lines via the aryl hydrocarbon receptor pathway.

Authors:

Jayne Gilbert, Geoffry N De Iuliis, Mark Tarleton, Adam McCluskey and Jennette A Sakoff

Laboratory of origin: J.A.S

Experimental Therapeutics Group, Department of Medical Oncology, Calvary Mater Newcastle Hospital, Edith Street, Waratah, 2298, NSW, Australia (J.G., J.A.S.).

Priority Research Centre for Reproductive Science, Faculty of Science, The University of Newcastle, University Drive, 2308, NSW, Australia (G.N.D).

Chemistry, School of Environmental & Life Sciences, Faculty of Science, The University of Newcastle, University Drive, Callaghan, 2308, NSW, Australia (M.T., A.M., J.A.S.).

Molecular Pharmacology Fast Forward. Published on December 21, 2017 as DOI: 10.1124/mol.117.109827
This article has not been copyedited and formatted. The final version may differ from this version.

Running Title: ANI-7 selectively targets breast cancer cell lines

Corresponding Author: Jennette A. Sakoff, Experimental Therapeutics Group, Department of Medical Oncology, Calvary Mater Newcastle Hospital, Edith Street, Waratah, NSW, Australia, 2298. Tel: (61) 2 40143560; Fax (61) 2 49680384; E-mail: jennette.sakoff@newcastle.edu.au

Number of text pages: 25

Number of tables: 4

Number of references: 45

Number of Words in:

Abstract: 239

Introduction: 635

Discussion: 1499

Abbreviations:

ANI-7, (*Z*)-2-(3,4-dichlorophenyl)-3-(1*H*-pyrrol-2-yl)acrylonitrile; AhR, aryl hydrocarbon receptor; TN, triple negative; ER, estrogen receptor; PR, progesterone receptor; HER2, human epidermal growth factor receptor; PAH, polycyclic aromatic hydrocarbon; HAH, halogenated aromatic hydrocarbon; Hsp90, heat-shock protein 90; p23, prostaglandin E synthase 3; XAP2, immunophilin-like protein hepatitis B virus X associated protein 2; ARNT, AhR nuclear translocator; XRE, xenobiotic response elements; CYP, cytochrome p450; EGFR, epidermal growth factor receptor; SULT, sulphur transferase; DMSO, dimethylsulfoxide; DMEM, Dulbecco's modified Eagle's medium; MTT, 3-(4,5-dimethylthiazol-2-yl)-2,5-diphenyltetrazolium bromide; PBS, phosphate buffered saline.

Molecular Pharmacology Fast Forward. Published on December 21, 2017 as DOI: 10.1124/mol.117.109827
This article has not been copyedited and formatted. The final version may differ from this version.

Abstract

We have previously reported the synthesis and breast cancer selectivity of (*Z*)-2-(3,4-dichlorophenyl)-3-(1*H*-pyrrol-2-yl)acrylonitrile (ANI-7) in cancer cell lines. To further evaluate the selectivity of ANI-7 we have expanded upon the initial cell line panel to now include the breast cancer cell lines (MCF7, MCF7/VP16, BT474, T47D, ZR-75-1, SKBR3, MDA-MB-468, BT20, MDA-MB-231), normal breast cells (MCF-10A) and cell lines derived from colon (HT29), ovarian (A2780), lung (H460), skin (A431), neuronal (BE2C), glial (U87, SJG2), and pancreatic (MIA) cancers. We now show that ANI-7 is up to 263-fold more potent at inhibiting the growth of breast cancer cell lines (MCF7, MCF7/VP16, BT474, T47D, ZR-75-1, SKBR3, MDA-MB-468), than normal breast cells (MCF-10A) or cell lines derived from other tumour types. Measures of growth inhibition, cell cycle analysis, morphological assessment, western blotting, receptor binding, gene expression, siRNA technology, reporter activity and enzyme inhibition assays were exploited to define the mechanism of action of ANI-7. Herein, we report that ANI-7 mediates its effects via the activation of the aryl hydrocarbon receptor (AhR) pathway and the subsequent induction of CYP1 metabolising monooxygenases. The metabolic conversion of ANI-7 induces DNA damage, checkpoint activation, S-phase cell cycle arrest and cell death in sensitive breast cancer cell lines. Basal expression of AhR, the nuclear transporter ARNT, and the CYP1 family members do not predict for sensitivity; however, inherent expression of the phase II metabolising enzyme SULT1A1 does. For the first time we identify (*Z*)-2-(3,4-dichlorophenyl)-3-(1*H*-pyrrol-2-yl)acrylonitrile as a new AhR ligand.

Molecular Pharmacology Fast Forward. Published on December 21, 2017 as DOI: 10.1124/mol.117.109827
This article has not been copyedited and formatted. The final version may differ from this version.

Introduction

Breast cancer is the most common cancer in women both in the developed and less developed world and the incidence is on the rise. Early stage breast cancer treatments include surgery and radiotherapy, while chemotherapy, hormonal and targeted therapies are considered for more aggressive tumours. Tamoxifen and anastrozole are standard treatment for hormone sensitive tumours; however drug resistance is often induced and tumour selectivity is poor (Ma et al., 2015). Herceptin, selectively targets the human epidermal growth factor receptor (HER2); however 70 % of HER2 positive patients fail to respond to treatment, with resistance developing rapidly. Herceptin also induces significant cardiac dysfunction in 2-7 % of patients. Even fewer options are available for triple negative tumours (TN) that are receptor negative for estrogen (ER), progesterone (PR) and HER2. TN breast cancers are vastly heterogeneous hindering targeted therapy development (Sharma, 2016). Critically and irrespective of the hormonal status, 33 % of patients with initial breast cancer experience recurrence or metastasis, while 5 % of new breast cancer patients present with metastases at diagnosis. The 5-year survival for these advanced breast cancer patients is only 25 % and despite all efforts metastatic breast cancer remains incurable (Steeg, 2016). The need to identify better therapies and translate these discoveries into the clinic has never been greater.

We have previously reported the synthesis of (*Z*)-2-(3,4-dichlorophenyl)-3-(1*H*-pyrrol-2-yl)acrylonitrile (ANI-7, Figure 1A) and identified it as a potent and selective inhibitor of cell growth in MCF-7 breast cancer cells (Tarleton et al., 2011), while having minimal to no effect on the growth of normal non-tumour derived breast cells or cells derived from other tumour types including colon, ovarian, lung, skin, neuronal, glial, and pancreatic. Spurred on by this discovery we set out to investigate the breast cancer selectivity of ANI-7 and to identify its mode-of-action using standard cell-based technologies. Herein we compare the growth inhibition qualities of ANI-7 with other structurally comparable analogues and standard breast cancer treatments (Figure 1), in a broader cell line panel and report that ANI-7 mediates its breast cancer selective effects via the aryl hydrocarbon receptor (AhR) pathway.

Molecular Pharmacology Fast Forward. Published on December 21, 2017 as DOI: 10.1124/mol.117.109827
This article has not been copyedited and formatted. The final version may differ from this version.

The AhR is a member of the basic-helix-loop-helix transcription factor family and is commonly known for its ability to mediate the effects of polycyclic (PAH) and polyhalogenated aromatic hydrocarbon (HAH) ligands including environmental toxins (Androutsopoulos et al., 2009; Kolluri et al., 2017; Okey, 2007; Walsh et al., 2013). However, many endogenous ligands also exist including bilirubin, prostaglandins, tryptophan and even plant derived ligands such as resveratrol and flavones (Murray et al., 2014; Tian et al., 2015). As more evidence becomes available the complexity of the AhR pathway is ever increasing, indeed the AhR can influence gene transcription and various cellular events even in the absence of ligand binding (Barhoover et al., 2010; Murray et al., 2014).

The AhR is constitutively localized within the cell cytosol where it is part of a complex of two heat-shock proteins: heat-shock protein 90 (Hsp90), prostaglandin E synthase 3 (p23) and a single molecule of the immunophilin-like protein hepatitis B virus X associated protein 2 (XAP2). This chaperone complex protects the AhR from degradation, constrains the AhR in a conformation receptive to ligand binding and prevents the inappropriate binding of the AhR nuclear translocator (ARNT) (Androutsopoulos et al., 2009; Denison and Nagy, 2003; Okey, 2007). Ligand binding to the AhR triggers a conformational change that exposes a nuclear localisation sequence that facilitates ARNT binding and translocation to the nucleus. Within the nucleus, the AhR:ARNT heterodimer complex binds to specific DNA recognition sites known as xenobiotic response elements (XREs), leading to the transcriptional activation of genes that possess XRE in their promotor sequences. AhR activated genes encode phase I metabolic enzymes such as cytochrome p450 (CYP) CYP-1A1, -1A2 and -1B1. The unliganded AhR is then exported back to the cytosol (Androutsopoulos et al., 2009; Okey, 2007).

Molecular Pharmacology Fast Forward. Published on December 21, 2017 as DOI: 10.1124/mol.117.109827
This article has not been copyedited and formatted. The final version may differ from this version.

Materials and Methods

Growth Inhibition

All test agents were prepared as stock solutions (20 mM) in dimethyl sulfoxide (DMSO) and stored at -20 °C. Tamoxifen, 4-hydroxytamoxifen, Anastrozole, CH223191, Raloxifene, Tyrphostin and α-naphthoflavone were purchased from Sigma. Aminoflavone was obtained from the NCI, USA. Cell lines used in the study included MCF-7, MDA-MB-468, T47D, ZR-75-1, SKBR3, BT474, BT20, MDA-MB-231, MCF7/VP16 (breast carcinoma); HT29 (colorectal carcinoma); U87, SJ-G2, SMA (glioblastoma); A2780 (ovarian carcinoma); H460 (lung carcinoma); A431 (skin carcinoma); Du145 (prostate carcinoma); BE2-C (neuroblastoma); and MiaPaCa-2 (pancreatic carcinoma) together with the one non-tumour derived normal breast cell line (MCF10A). All cell lines were incubated in a humidified atmosphere 5 % CO_2 at 37 °C. The cancer cell lines MCF7, MCF7/VP16, MDA-MB-231, HT29, U87, SJ-G2, SMA, A2780, H460, A431, DU145, BE2-C and MIAPaCa2 were maintained in Dulbecco's modified Eagle's medium (DMEM; Sigma, Australia) supplemented with foetal bovine serum (10 %), sodium pyruvate (10 mM), penicillin (100 $IUmL^{-1}$), streptomycin (100 μgmL^{-1}), and L-glutamine (2 mM). The cancer cell lines MDA-MB-468, T47D, ZR-75-1, SKBR3 and BT474 were maintained in RPMI-1640 (Sigma, Australia) supplemented with foetal bovine serum (10 %), sodium pyruvate (10 mM), penicillin (100 $IUmL^{-1}$), streptomycin (100 μgmL^{-1}), L-glutamine (2 mM) and HEPES (10 mM). The non-cancer MCF10A cell line was maintained in DMEM:F12 (1:1) cell culture media, 5 % heat inactivated horse serum, supplemented with penicillin (50 $IUmL^{-1}$), streptomycin (50 μgmL^{-1}), HEPES (20 mM), L-glutamine (2 mM), epidermal growth factor (20 $ngmL^{-1}$), hydrocortisone (500 $ngmL^{-1}$), cholera toxin (100 $ngmL^{-1}$), and insulin (10 $mgmL^{-1}$). Cytotoxicity was determined by plating cells in duplicate in medium (100 µL) at a density of 2500–4000 cells per well in 96-well plates. On day 0 (24 h after plating), when the cells are in logarithmic growth, medium (100 µL) with or without the test agent was added to each well. After 72 h drug exposure, growth inhibitory effects were evaluated using the MTT (3-(4,5-dimethyltiazol-2-yl)-2,5-diphenyltetrazolium bromide) assay and absorbance read at 540 nm. An eight-point dose-response curve was produced as shown in Figure 2 using MS Excel software. Each data point is the mean ± the standard error of the mean (SEM) calculated from 4-5 replicates

Molecular Pharmacology Fast Forward. Published on December 21, 2017 as DOI: 10.1124/mol.117.109827
This article has not been copyedited and formatted. The final version may differ from this version.

which were performed on separate occasions and separate cell line passages. From these dose response curves the GI_{50} value was calculated, representing the drug concentration at which cell growth was inhibited by 50 % based on the difference between the optical density values on day 0 and those at the end of drug exposure (Tarleton et al., 2011).

Cell Cycle Analysis

Tumour cells in logarithmic growth were transferred to 6 well plates at a density of $2x10^5$-$2.5x10^5$ cells/ well. On day 0 (24 h after plating), the cells were treated with or without the test agent. The cells were harvested 24 h after drug treatment and washed twice in phosphate buffered saline (PBS), fixed in 70 % ethanol and stored overnight at -20 °C. The cell pellet was incubated in 600 µl of PBS containing propidium iodide (40 μgmL^{-1}) and RNase (200 μgmL^{-1}) for at least 30 min at room temperature. The samples ($1.5x10^4$ events) were analysed for fluorescence (FL2 detector, filter 575/30 nm band pass) using a FACScan (Becton Dickinson). Cell cycle distribution was assessed using Cell Quest software. Experiments were each performed on three separate occasions. Values are the percentage distribution for each phase of the cell cycle.

Morphological Assessment

Live cells were examined for morphological alterations after 24 h exposure with and without ANI-7, using phase contrast microscopy (Olympus CKX41 inverted microscope 100x magnification)(Supplemental Figure 1).

Western Blotting

Cells ($3x10^5$) were plated in 6 well plates in DMEM media containing test agent. At the indicated times the cells were harvested and protein content determined (Lowry Modified/Biorad Protein Assay). Equal aliquots (20 µg) of total protein from whole cell lysates were fractionated on a 10 % denaturing sodium dodecyl sulfate (SDS) polyacrylamide gel and transferred to polyvinylidine difluoride membranes. Nonspecific interactions were blocked with 5 % nonfat milk/0.05 % Tween 20. Proteins

Molecular Pharmacology Fast Forward. Published on December 21, 2017 as DOI: 10.1124/mol.117.109827
This article has not been copyedited and formatted. The final version may differ from this version.

were identified using rabbit monoclonal antibodies against gamma H2AXγ, and pCHK2 (Cell signaling) and mouse monoclonal antibody CHK2. Membrane-bound antibodies were detected using goat anti-rabbit and anti-mouse secondary antibodies (Abcam) and Clarity Western ECL (Bio-Rad).

ER Binding

Competition binding assays were performed by using an enzyme fragment complementation (EFC) method described in the HitHunter (Freemont, CA) EFC Estrogen Chemiluminescence Assay kit according to the manufacturer's instructions. Briefly, competing ligands at final concentrations ranging from 25 pM to 2 µM were incubated with 5 nM recombinant ERα (Invitrogen) and 17β-estradiol-conjugated enzyme donor for 1.5 h. The enzyme acceptor was then added followed by the chemiluminescence substrate and incubated for 1 h. Relative luminescence was determined by using a GloMax Explorer plate reader (Promega). Sigmoidal standard curves were created by Excel.

Aromatase Assay

Aromatase reactions were carried out as previously described (Matsui et al., 2005). Test chemicals were dissolved in DMSO and diluted 1:10 in Diluent 1 (0.1 % BSA, 50 mM phosphate buffer (PB), pH7.2). Sample (10 µL) was added to a 96-well plate (on ice) followed by 50 µL of ice-cold R1 solution (0.1 % BSA, 50 mM PB, pH 7.2, 3.3 mM NADP-2Na, BD Biosciences), 0.8 µM glucose-6-phosphate and 62.5 nM testosterone (Sigma). R2 solution (50 µL, 0.1 % BSA, 50 mM PB, pH 7.2, 8.3 mM magnesium chloride and 1UmL^{-1} glucose-6-phosphate dehydrogenase) was added to each test sample. 10 µL diluted P450arom (1 pg/ml, 0.1 % BSA, 50 mM PB, pH7.2, BD Biosciences) was added to a second 96-well plate on ice. 90 µl of sample reaction was transferred to the P450arom and incubated for 20 min at 37 °C. The reaction was terminated with 10 µL of 500 µM α-naphthoflavone. After completion of the P450aromatase reaction, 50 µL of sample was transferred to an ELISA plate. The amount of estradiol in each sample was determined using the Estradiol EIA kit (Cayman Chemical Company, Ann Arbor) according to the manufacturer's instructions. Absorbance of each sample was

Molecular Pharmacology Fast Forward. Published on December 21, 2017 as DOI: 10.1124/mol.117.109827
This article has not been copyedited and formatted. The final version may differ from this version.

proportional to the amount of bound estradiol tracer which was inversely proportional to the amount of estradiol.

Kinase Inhibition

A dry sample of ANI-7 was sent to Reaction Biology Corp (PA, USA) and The International Centre for Kinase Profiling (The University of Dundee, UK) for kinase inhibition assays. Both organisations use the ^{33}P ATP radioactive filter binding assay(Hastie et al., 2006). A stock solution of ANI-7 was prepared in DMSO and kinase inhibition assays were conducted in duplicate in the presence of a single concentration of ANI-7 (10 µM). Data represents percentage kinase enzyme activity, the lower the value the greater the enzyme inhibition.

Knockdown of AhR Expression

Transient knockdown of AhR in MDA-MB-468 cells was performed through transfection of small interfering RNAs (siRNA) targeting AhR (Qiagen) and the AllStars Negative Control nonsilencing siRNA (Qiagen). The AhR siRNA contained four siRNAs for the AhR target (FlexiTube GeneSolution GS196). Cells were transfected with Lipofectamine 3000 (Invitrogen) according to the manufacturer's instructions. Briefly, 8x10^3 MDA-MB-468 cells were plated into each well of a 96-well plate and allowed to adhere for 24 h. Opti-MEM media (Invitrogen) containing 0.3 ml of Lipofectamine 3000 transfection reagent and 0.3 pmol siRNA was added to each well. After 6 h of incubation, transfection media was replaced with growth media containing 1.0 µM ANI-7. Cells were incubated for a further 72 h prior to MTT analysis.

AhR Reporter Luciferase Assay

The activity of the AhR signalling pathway was measured using the Cignal Xenobiotic Response (XRE) Reporter Assay Kit from Qiagen according to the manufacturer's instructions. Briefly, MDA-MB-468 cells were reverse transfected with the Cignal XRE Reporter (containing an AhR-responsive luciferase construct and a constitutively expressing Renilla luciferase) as well as positive and negative controls. After 20 h of transfection, medium was changed to assay medium (DMEM +

Molecular Pharmacology Fast Forward. Published on December 21, 2017 as DOI: 10.1124/mol.117.109827
This article has not been copyedited and formatted. The final version may differ from this version.

0.5% FBS +0.1 mM NEAA). After 24 h of transfection, cells were treated with ANI-7 (0.2 µM and 2.0 µM) for 6 h. The Dual-Glo Luciferase Assay System (Promega) was performed after 30 h of transfection using the GloMax Explorer Luminescence plate reader. The promoter activity was replicated twice and values are expressed as arbitrary units using Renilla reporter for internal normalization.

Gene Expression Analysis

For each cell population total RNA was extracted using the RNeasy Mini Kit (Qiagen) according to the manufacturer's instructions. One µg of RNA was reverse transcribed using the QuanitTect Reverse Transcription Kit (Qiagen) according to the manufacturer's instructions. Rotor-Gene SYBR Green PCR Kit (Qiagen) was used to perform qPCR for AhR, CYP1A1, CYP1A2, CYP1B1, SULT1A1 and ARNT on a Rotor-Gene 3000 Thermo -Cycler Instrument using β_2-microglobulin as a housekeeping gene (Qiagen). The primer sequences were purchased from Qiagen as follows: AhR (QT02422938), CYP1A1 (QT00012341), CYP1A2 (QT00000917), CYP1B1 (QT00209496), SULT1A1 (QT01665489), ARNT (QT00023177) AND β_2M (QT00088935). HotStar Taq activation at 95^{o}C for 5 minutes, 40 cycles of denaturation (95^{o}C for 5 seconds), and annealing/extension (60^{o}C for 10 seconds). The comparative C_t value method was used for data analysis. Endogenous gene expression was examined in cell harvests from each of our cell lines; while ANI-7 induced gene expression was examined in MDA-MB-468 cells following treatment with 2 µM ANI-7 for 1, 2, 4, 8, 12 and 24 h.

Results

ANI-7 selectively targets breast cancer cell populations

We have previously shown that ANI-7 induces potent selective growth inhibition in MCF-7 breast cancer cells (GI_{50} = 0.5 µM) when compared to cell lines derived from other tumour types (GI_{50} = 3.2 - 46 µM)(Tarleton et al., 2011). At the time of this discovery the mechanism-of-action of ANI-7 was unknown and the selectivity was only examined in a limited number of breast cancer cell lines (MCF-7

Molecular Pharmacology Fast Forward. Published on December 21, 2017 as DOI: 10.1124/mol.117.109827
This article has not been copyedited and formatted. The final version may differ from this version.

and MDA-MB-231). In the present study, we set out to compare the action of ANI-7 with other well-known breast cancer targeting drugs (Figure 1) and to expand the panel of breast cancer cell lines to now include cells lines of ER+ luminal A (MCF-7, T47-D and ZR-75-1 cells), ER+ luminal B (BT-474 cells), HER2+ (SKBR-3), Basal (triple negative for ER,PR and HER2; MDA-MB-468, BT20 and MDA-MB-231 cells), and MCF-7/VP16 cells which overexpresses the drug resistance ABCC1 gene. The results of our extended growth inhibition analysis clearly shows that ANI-7 potently inhibits the growth of not only MCF-7 breast cancer cells but also other breast cancer derived cell lines (Figure 2, solid lines), while showing negligible activity in a broad range of non-breast derived cell lines (dashed lines). Indeed comparisons of the GI_{50} values (Table 1) show that ANI-7 produces a GI_{50} value of 0.38 ± 0.03 μM in MCF-7 cells while values of 3.0 – 42 μM were observed in cell lines from lung, colon, ovary, neuronal, glial, prostate, and pancreas. The only other tumour type that showed appreciable growth inhibition by ANI-7 was the A431 vulva cell line (GI_{50} = 0.51 ± 0.05 μM).

Comparison with other well-known breast cancer targeting drugs show that the ER antagonists tamoxifen, its metabolite hydroxy tamoxifen, and raloxifene did not selectively inhibit the growth of MCF-7 (GI_{50} = 7.7 ± 0.6, 4.2 ± 1.2 and 8.7 ± 3.3 μM, respectively) cells when compared with cell lines derived from other tumour types (GI_{50} range, 6.5 – 18, 2 – 9.5 and 11 – 21 μM, respectively). Although the aromatase inhibitor, anastrozole, showed a slight preference for MCF-7 cells (GI_{50} = 35 ± 16 μM vs >50 μM), it was essentially ineffective at inhibiting cell growth in this model system. Similarly, the EGFR inhibitor Tyrphostin RG14620 also failed to show any selective preference towards the growth inhibition of MCF-7 cells (GI_{50} = 12 ± 1 μM vs a range of 5.8 – 18 μM). However, in contrast with these standard breast cancer treatments, the aryl-hydrocarbon agonist, aminoflavone mimicked the breast cancer selectivity of ANI-7 with a GI_{50} value of 0.006 ± 0.001 μM in MCF-7 cells and a GI_{50} range of 0.16 – 21 μM in all other cell types.

In our expanded breast cancer panel (Table 2), ANI-7 potently inhibited the growth of T47D, ZR-75-1, MCF-7, SKBR3, and MDA-MB-468 breast cancer cells (GI_{50} range of 0.16 – 0.38 μM), moderately inhibited the growth of BT20 and BT474 cells (GI_{50} range of 1-2 μM) and essentially failed to inhibit the growth of MDA-MB-231 and MCF10A cells (GI_{50} range of 17-26 μM). Moreover, ANI-7 maintained its

Molecular Pharmacology Fast Forward. Published on December 21, 2017 as DOI: 10.1124/mol.117.109827
This article has not been copyedited and formatted. The final version may differ from this version.

ability to inhibit the growth of drug resistant cells (MCF-7/VP16: GI_{50} = 0.21 ± 0.4 μM). Tamoxifen, hydroxytamoxifen and raloxifene produced GI_{50} values of 4.7 – 9.7, 3.1 – 12 and 7.2 – 20 μM respectively, with T47D cells the most sensitive and the MDA-MB-231 the least sensitive of the breast cancer cell lines. Anastrozole again induced minimal effects on growth inhibition across all cell lines (GI_{50} range 22 to >50 μM), while Tyrphostin RG14620 induced moderate inhibition (GI_{50} 8.5 - 17 μM). Although aminoflavone was more potent than ANI-7, it again mimicked the response of ANI-7 producing GI_{50} range of 0.001 - 0.04 μM in T47D, ZR-75-1, MCF-7, SKBR3 and MDA-MB-468 cells, moderate inhibition in BT474 and BT20 (GI_{50} range of 0.8 -7.0 μM) and minimal effects in MDA-MB-231 and MCF10A (GI_{50} range of 16 - 20 μM) cells.

ANI-7 induces cell cycle arrest checkpoint activation and DNA damage

In order to further investigate the mode-of-action of ANI 7 we chose to focus on the cell cycle events induced in MDA-MB-468 cells in response to ANI-7. Cell cycle analysis (Figure 3) and morphological assessment (Supplemental Figure 1) of ANI-7 confirmed the negligible effect of ANI-7 (2.5 μM) on the growth of normal breast MCF10A cells within 24h (Figure 3A-B), while ANI-7 induced significant S-phase and G_2 + M phase cell cycle arrest within 24 h of treatment in MDA-MB-468 cells (Figure 3C-D). Western blot analysis confirmed the induction of cell cycle checkpoint activation within 12 h of treatment with ANI-7 (2 μM) in MDA-MB-468 cells, via a significant increase in the content and phosphorylation of CHK2 (25 fold increase) (Figure 4A). Concomitantly, ANI-7 (2 μM) induced a significant increase in H2AXɣ (3.5 fold increase) in MDA-MB-468 cells within the same timeframe, indicative of DNA double strand damage (Figure 4B). The ability of ANI-7 to selectively target breast cancer cells and to induce S-phase cell cycle arrest was the initial clue that led us to examine the role of ANI-7 in the aryl hydrocarbon receptor pathway as similar events have been described for aminoflavone (Meng et al., 2006).

Inhibition of the AhR pathway ameliorates the effects of ANI-7

Using the MTT growth inhibition assay we observed that treatment of MDA-MB-468 cells with CH223191 (5 µM), a known antagonist of the AhR (Choi et al., 2012), significantly reduced the growth inhibitory effects of both ANI-7 (0.1 µM)(from 60% to 17 % relative growth inhibition) and aminoflavone (3 pM) (from 100 % to 28 % relative growth inhibition) (Figure 5A). As the AhR pathway is also known to induce the expression of phase 1 metabolising enzymes including cytochrome P450 (CYP1) enzymes, we also observed that the specific CYP1 inhibitor α-naphthoflavone (10 µM) ameliorated the growth inhibitory effects of both ANI-7 (0.5 µM) and aminoflavone (3 pM) from near total growth inhibition to negligible growth inhibition (Figure 5B). Further to this, siRNA knockdown of AhR expression (by 60%, Figure 5C) in MDA-MD-468 cells enhanced the survival of cells from 26 % to 57 % following treatment with ANI-7 (1 µM)(Figure 5D). Collectively, this data confirms the role of the AhR and CYPs in mediating the effects of ANI-7 pathway.

ANI-7 activates XRE activity and expression of the AhR and CYP1 members

The ability of ANI-7 to induce binding of the AhR with the XRE promotor was determined using a XRE reporter assay. The ANI-7 sensitive cell line MDA-MB468 was transfected with an XRE reporter plasmid, as well as control reporter plasmids. Treatment with ANI-7 at concentrations of 0.2 and 2.0 µM significantly induced promotor activity by up to 2 fold within 6 h (Figure 6A), confirming XRE activation. Treatment of these cells with ANI-7 also induced a modest increase in the expression of AhR by up to 3.6-fold within 24 h (Figure 6B). Analysis of CYP1A1 expression over the same 24 h exposure showed a 28-fold increase in CYP1A1 expression within 1 h reaching a maximum fold increase of 252 by 8h post treatment (Figure 6C). CYP1A2 and CYP1B1 also showed an increase in expression within 1h of treatment reaching a maximum fold increase of 21 and 13 by 12 h post treatment, respectively (Figure 6D and 6E). Interestingly, the expression of SULT1A1 did not alter following treatment with ANI-7 (Figure 6F). To further define the role of the AhR pathway in mediating the effects of ANI-7 we examined the basal expression of AhR, ARNT, CYP1 family and SULT1A1 in our large panel of cell lines (Figure 7A-F) and compared the expression with ANI-7 sensitivity (Figure 2). Interestingly the cell

Molecular Pharmacology Fast Forward. Published on December 21, 2017 as DOI: 10.1124/mol.117.109827
This article has not been copyedited and formatted. The final version may differ from this version.

lines displayed a varying profile of gene expression of the key members of the AhR pathway. Of note, the inherent expression of AhR, ARNT and CYP1 members did not predict for ANI-7 activity; however, SULT1A1 expression did. Collectively, the data shows that ANI-7 is mediating its effects via the AhR pathway with a particular enhancement of CYP1A1 expression.

ANI-7 does not interact with other standard breast cancer targets

During our initial investigations into the mechanism-of-action we also examined the ability of ANI-7 to interact with the ER pathway. Thus, we examined the ability of ANI-7 to bind to the ER and to inhibit aromatase activity. The data in Table 3, clearly shows that while tamoxifen (IC_{50} 0.012 µM) and hydroxytamoxifen (IC_{50} 0.0017 µM) are potent inhibitors of ER and anastrazole (IC_{50} 0.12 µM) is a potent inhibitor of aromatase activity, ANI-7 failed to inhibit either target at concentrations 1000 times greater than the IC_{50} values for these targeted therapies. In order to further characterise the activity of ANI-7 we also screened its ability to inhibit the activity of a panel of protein kinases at a concentration of 10 µM (Table 4). The data clearly shows that ANI-7 does not significantly alter the kinase activity of a very broad panel of kinase enzymes, including tyrosine kinase receptors, lipid kinases, or those specific to the PI3K/mTOR or MAP Kinase pathway.

Discussion

Herein we report that (*Z*)-2-(3,4-dichlorophenyl)-3-(1*H*-pyrrol-2-yl)acrylonitrile (ANI-7) is a potent (µM) and selective (up to 263-fold) inhibitor of cell growth in breast cancer cell lines (Figure 2, Tables 1-2). The sensitive lines represent cancers from the main molecular subtypes of luminal A (MCF-7, T47D, ZR-75-1), luminal B (BT474), basal (MDA-MB-468, BT20) and HER2 (SKBR3) with varying receptor status (ER, PR, HER2)(Table 2). Also included is one line with a drug resistant phenotype (MCF-7/VP16), overexpressing the p-glycoprotein drug transporter ABCC1. Interestingly, all ER positive lines

Molecular Pharmacology Fast Forward. Published on December 21, 2017 as DOI: 10.1124/mol.117.109827
This article has not been copyedited and formatted. The final version may differ from this version.

were sensitive to growth inhibition by ANI-7. Of the ER negative cell lines, the MDA-MB-468 line was the most sensitive. Sensitivity of this cell line and other ER negative cells to AhR ligands has previously been described (Bradshaw et al., 2008; Brinkman et al., 2014; Zhang et al., 2009). The only non-sensitive breast cancer cell line was the MDA-MB-231 line with a basal subtype and triple negative for receptor status, with amplifying mutations in KRas and BRaf activity (Eckert et al., 2004). While these mutations are relatively common in colon cancer less than 5% of breast cancer tumours carry this genotype (Bos, 1989). The resistance of MDA-MB-231 to AhR activation has been observed with other AhR ligands including aminoflavone (Callero and Loaiza-Perez, 2011; Fukasawa et al., 2015). The only other tumour type that showed appreciable sensitivity to ANI-7 was the A431 vulva cell line, which is ER positive and overexpresses the EGFR growth receptor (Rexer et al., 2009). Initially our investigations were focused on the possibility that ANI-7 was a selective inhibitor of ER+ cell populations (Tarleton et al., 2011), however it became clear that ANI-7 was not a ligand for the ER or a substrate for aromatase function (Table 3). ANI-7 also failed to inhibit a broad range of kinase activity (Table 4), further excluding ANI-7 from mediating its effects by traditional breast cancer related biochemical pathways including the EGFR/HER2, PI3K/mTOR, and MAP kinase pathways. We also show that the growth inhibition profile of ANI-7 differs considerably from that induced by ER (tamoxifen, hydroxytamoxifen, raloxifene), aromatase (anastrozole) and EGFR (tyrphostin) antagonism.

Our desire to determine the mode-of-action of ANI-7 led us to examine the effect of ANI-7 on the cell cycle (Figure 3) whereby ANI-7 induced S-phase cell cycle arrest. This single observation led us to examine the possibility that ANI-7 was mediating its effects as described for the halogenated aryl hydrocarbon, aminoflavone (Meng et al., 2005); i.e via activation of the AhR pathway. Aminoflavone was first described by Akama et al (Akama et al., 1996) as a selective inhibitor of the growth of breast cancer cells. Subsequent studies have shown that the selectivity of aminoflavone relies on the localisation of the AhR in the cytoplasm rather than the nucleus of cells (Callero and Loaiza-Perez, 2011). Structurally aminoflavone can be metabolised by CYP1A1 at two amino groups to form N-hydroxyl metabolites that are substrates for bioactivation by sulphur transferase (SULT1A1) (Meng et al., 2006). N-sulfoxy groups are further converted to active nitrenium ions, which form DNA adducts

and induce cell death (Meng et al., 2006). The ability of aminoflavone to be metabolised at two amino groups compared with ANI-7's single amino group may account for their differing potency. Although aminoflavone presents with greater potency (Table 2), this does not preclude the development of ANI-7 as a new clinical lead. Indeed, highly potent molecules are often difficult to detect in blood and present with a narrow therapeutic index with unpredictable toxicity, off-targets and poor pharmacokinetics; ie high potency does not necessarily equate with greater clinical efficacy (Waldman, 2002).

Using standard cell biology methods we show that ANI-7 binds to the AhR, induces translocation to the nucleus, activates the XRE (Figure 6A), induces CYP1 activity (Figure 6C-E), culminating in cell cycle arrest (Figure 3), checkpoint activation (Figure 4A), DNA damage (Figure 4B) and cell death (Figure 2 and supplemental data Figure 1). Of note, is the significant induction of CYP1 expression within 1 hour following treatment, with CYP1A1 dominating the effect (Figure 6C). Although, ANI-7 clearly mediates its effects via the AhR pathway, the inherent expression of each pathway member (AhR, ARNT, and CYP1)(Figure 7) does not predict for sensitivity, highlighting the well-known inducible nature of this pathway rather than constitutive activity. In contrast, the inherent expression of SULT1A1 did predict for ANI-7 sensitivity and its expression was not altered following treatment, indicating that it functions independently of the AhR pathway. Notwithstanding this, the role of SULT1A1 is clearly an important determinant for the breast cancer selectivity of ANI-7. Studies of aminoflavone activity and gene expression in NCI-60 cell line panel (National Cancer Institute Developmental Therapeutics Program) showed that selectivity was highly correlated with the expression of SULT (Meng et al., 2006). Moreover, the transfection of SULT1A1 into MDA-MB-231 aminoflavone-resistant cells restored sensitivity (Meng et al., 2006).

In the present study we also show that the growth inhibitory effect of ANI-7 is ameliorated in the presence of the AhR antagonist CH223191 (Choi et al., 2012), AhR siRNA (Figure 5A, C-D) and the pan CYP1 inhibitor αNF (Figure 5B) confirming the need for each step of the AhR pathway and the metabolism of ANI-7 to an active intermediary. The presence of the DNA damage marker γH2AX and the cell cycle checkpoint activation suggest that ANI-7 is metabolised to a DNA interacting compound. Although we have not identified the precise ANI-7 metabolites, it is likely that the amino group of ANI-7

Molecular Pharmacology Fast Forward. Published on December 21, 2017 as DOI: 10.1124/mol.117.109827
This article has not been copyedited and formatted. The final version may differ from this version.

is metabolised to an active nitrenium ion as observed for aminoflavone. Furthermore, the sensitivity of the cell lines to ANI-7 and the induction of DNA damage are independent of their p53 status, ie MCF-7 (sensitive) and MCF10A (insensitive) cells are both p53 wildtype; while MDA-MB-468 (sensitive), and MDA-MB-231 (insensitive) are p53 mutant.

Other halogenated aryl-hydrocarbon molecules have been shown to selectively target breast cancer cells via activation of the AhR pathway (Callero and Loaiza-Perez, 2011; Fukasawa et al., 2015; Loaiza-Perez et al., 2002) including 2-(4-amino-3-methylphenyl)-5-fluorobenzothiazole (5F-203) and (5S,7S)-7-methyl-3-(3-(trifluoromethyl)phenyl)-5,6,7,8-tetrahydrocinnolin-5-ol (NK150460). Of note, the amino containing compound 5F-203 has been shown to induce S-phase accumulation and DNA-adduct formation (Trapani et al., 2003). In contrast, the non-amino containing compound, NK150460, failed to induce γH2AX expression, indicating that DNA-adduct formation was not induced (Fukasawa et al., 2015). Not surprisingly, the initial chemical scaffold clearly dictates the structure and function of active metabolites produced via this pathway.

Other acrylonitrile compounds ((*Z*)-2,3-bis(4-nitrophenyl)acrylonitrile) (ZNPA) have been shown to activate the AhR including its translocation to the nucleus; however, ZNPA does not activate CYP1 expression in cell models (Guyot et al., 2012). Thus, while halogenated aryl-hydrocarbons and acrylonitrile compounds have been shown to activate the AhR pathway the specific steps and mechanisms do differ, underscoring the importance of characterising the mode of action. Exploring the differential effects of AhR agonists opens the way to exploit their subtle differences for the clinical treatment of disease including management of potential clinical toxicities which have been described for prodrugs of aminoflavone and 5F-203 (Behrsing et al., 2013; NIH-DCTD).

The AhR has been previously described in the initiation and progression of breast cancer (Go et al., 2015; Nebert et al., 2004; Powell et al., 2013; Schlezinger et al., 2006; Vinothini and Nagini, 2010). The metabolism of environmental toxins by the AhR leads credence to the proposal that the initial insult that caused the breast cancer was a fat soluble xenobiotic element that was metabolised to a DNA damaging compound. The ongoing hyper-activation of the AhR in breast cancers and its ability to

Molecular Pharmacology Fast Forward. Published on December 21, 2017 as DOI: 10.1124/mol.117.109827
This article has not been copyedited and formatted. The final version may differ from this version.

control many oncogenic pathways further suggests a role of AhR in progression of this disease. Of note, the AhR is known to control the transcription of the ER gene. The cross-talk between these two pathways is complex (Callero and Loaiza-Perez, 2011; Go et al., 2015; Safe and Wormke, 2003). Indeed it has been proposed that a complex of AhR-ARNT and AhR agonist may dimerize with an ERα-ER agonist complex leading to the elevated expression of CYP1A1 and CYP1B1 (Go et al., 2015). Such a proposal may explain our observation that all ER positive cell lines (n= 5) tested in our study were sensitive to ANI-7, however, we clearly show that inherent CYP1 expression is not related to ANI-7 sensitivity. Furthermore, various AhR ligands have been shown to induce the proteasome-dependent degradation of ERα protein (Wormke et al., 2000; Wormke et al., 2003) and also directly target E2-(estradiol) responsive gene promotors (Krishnan et al., 1995).

This study for the first time has identified (*Z*)-2- (3,4-dichlorophenyl)-3-(1*H*-pyrrol-2-yl)acrylonitrile as a new AhR ligand and a substrate for CYP1 metabolism culminating in DNA damage and growth inhibition in breast cancer cells. The unique structure of ANI-7 provides a new platform for the design and development of novel breast cancer selective molecules exploiting the activation of the AhR pathway and the induction of CYP1s. This pharmacophore substantially adds to the ever increasing development of novel AhR targeting molecules for the treatment of cancer (Callero et al., 2017; Fukasawa et al., 2015; Kolluri et al., 2017; Luzzani et al., 2017; Yurttas et al., 2015).

Authorship Contributions

Participated in research design: Sakoff, and McCluskey

Conducted experiments: Gilbert, De Iuliis, Tarleton

Contributed new reagents or analytic tools: Tarleton

Performed data analysis: Sakoff, Gilbert, McCluskey

Wrote or contributed to writing of the manuscript: Sakoff, Gilbert, McCluskey

References

Akama T, Shida Y, Sugaya T, Ishida H, Gomi K and Kasai M (1996) Novel 5-aminoflavone derivatives as specific antitumor agents in breast cancer. *J Med Chem* **39**: 3461-3469.

Androutsopoulos VP, Tsatsakis AM and Spandidos DA (2009) Cytochrome P450 CYP1A1: wider roles in cancer progression and prevention. *BMC Cancer* **9**: 187.

Barhoover MA, Hall JM, Greenlee WF and Thomas RS (2010) Aryl Hydrocarbon Receptor Regulates Cell Cycle Progression in Human Breast Cancer Cells via a Functional Interaction with Cyclin-Dependent Kinase 4. *Molecular Pharmacology* **77**: 195-201.

Behrsing HP, Furniss MJ, Davis M, Tomaszewski JE and Parchment RE (2013) In vitro exposure of precision-cut lung slices to 2-(4-amino-3-methylphenyl)-5-fluorobenzothiazole lysylamide dihydrochloride (NSC 710305, Phortress) increases inflammatory cytokine content and tissue damage. *Toxicol Sci* **131**: 470-479.

Bos JL (1989) ras oncogenes in human cancer: a review. *Cancer Res* **49**: 4682-4689.

Bradshaw TD, Stone EL, Trapani V, Leong C-O, Matthews CS, te Poele R and Stevens MFG (2008) Mechanisms of acquired resistance to 2-(4-Amino-3-methylphenyl)benzothiazole in breast cancer cell lines. *Breast Cancer Research and Treatment* **110**: 57-68.

Brinkman AM, Wu J, Ersland K and Xu W (2014) Estrogen receptor alpha and aryl hydrocarbon receptor independent growth inhibitory effects of aminoflavone in breast cancer cells. *BMC Cancer* **14**: 344.

Callero MA and Loaiza-Perez AI (2011) The role of aryl hydrocarbon receptor and crosstalk with estrogen receptor in response of breast cancer cells to the novel antitumor agents benzothiazoles and aminoflavone. *Int J Breast Cancer* **2011**: 923250.

Callero MA, Rodriguez CE, Solimo A, Bal de Kier Joffe E and Loaiza Perez AI (2017) The Immune System As a New Possible Cell Target for AFP 464 in a Spontaneous Mammary Cancer Mouse Model. *J Cell Biochem*.

Choi EY, Lee H, Dingle RW, Kim KB and Swanson HI (2012) Development of novel CH223191-based antagonists of the aryl hydrocarbon receptor. *Mol Pharmacol* **81**: 3-11.

Denison MS and Nagy SR (2003) Activation of the aryl hydrocarbon receptor by structurally diverse exogenous and endogenous chemicals. *Annu Rev Pharmacol Toxicol* **43**: 309-334.

Eckert LB, Repasky GA, Ulku AS, McFall A, Zhou H, Sartor CI and Der CJ (2004) Involvement of Ras activation in human breast cancer cell signaling, invasion, and anoikis. *Cancer Res* **64**: 4585-4592.

Fukasawa K, Kagaya S, Maruyama S, Kuroiwa S, Masuda K, Kameyama Y, Satoh Y, Akatsu Y, Tomura A, Nishikawa K, Horie S and Ichikawa Y (2015) A Novel Compound, NK150460, Exhibits Selective Antitumor Activity against Breast Cancer Cell Lines through Activation of Aryl Hydrocarbon Receptor. *Molecular Cancer Therapeutics* **14**: 343-354.

Go RE, Hwang KA and Choi KC (2015) Cytochrome P450 1 family and cancers. *J Steroid Biochem Mol Biol* **147**: 24-30.

Guyot E, Coumoul X, Chasse JF, Khallouki F, Savouret JF, Poirot M and Barouki R (2012) Identification of a new stilbene-derived inducer of paraoxonase 1 and ligand of the Aryl hydrocarbon Receptor. *Biochem Pharmacol* **83**: 627-632.

Hastie CJ, McLauchlan HJ and Cohen P (2006) Assay of protein kinases using radiolabeled ATP: a protocol. *Nat Protoc* **1**: 968-971.

Kolluri SK, Jin UH and Safe S (2017) Role of the aryl hydrocarbon receptor in carcinogenesis and potential as an anti-cancer drug target. *Arch Toxicol*.

Krishnan V, Porter W, Santostefano M, Wang X and Safe S (1995) Molecular mechanism of inhibition of estrogen-induced cathepsin D gene expression by 2,3,7,8-tetrachlorodibenzo-p-dioxin (TCDD) in MCF-7 cells. *Mol Cell Biol* **15**: 6710-6719.

Loaiza-Perez AI, Trapani V, Hose C, Singh SS, Trepel JB, Stevens MF, Bradshaw TD and Sausville EA (2002) Aryl hydrocarbon receptor mediates sensitivity of MCF-7 breast cancer cells to antitumor agent 2-(4-amino-3-methylphenyl) benzothiazole. *Mol Pharmacol* **61**: 13-19.

Luzzani GA, Callero MA, Kuruppu AI, Trapani V, Flumian C, Todaro L, Bradshaw TD and Loaiza Perez AI (2017) In Vitro Antitumor Effects of AHR Ligands Aminoflavone (AFP 464) and Benzothiazole (5F 203) in Human Renal Carcinoma Cells. *J Cell Biochem*.

Ma CX, Reinert T, Chmielewska I and Ellis MJ (2015) Mechanisms of aromatase inhibitor resistance. *Nat Rev Cancer* **15**: 261-275.

Matsui K, Nishii S and Oka M (2005) P450 aromatase inhibition assay using a competitive ELISA. *J Pharm Biomed Anal* **38**: 307-312.

Meng LH, Kohlhagen G, Liao ZY, Antony S, Sausville E and Pommier Y (2005) DNA-protein cross-links and replication-dependent histone H2AX phosphorylation induced by aminoflavone (NSC 686288), a novel anticancer agent active against human breast cancer cells. *Cancer Res* **65**: 5337-5343.

Meng LH, Shankavaram U, Chen C, Agama K, Fu HQ, Gonzalez FJ, Weinstein J and Pommier Y (2006) Activation of aminoflavone (NSC 686288) by a sulfotransferase is required for the antiproliferative effect of the drug and for induction of histone gamma-H2AX. *Cancer Res* **66**: 9656-9664.

Murray IA, Patterson AD and Perdew GH (2014) Aryl hydrocarbon receptor ligands in cancer: friend and foe. *Nat Rev Cancer* **14**: 801-814.

Nebert DW, Dalton TP, Okey AB and Gonzalez FJ (2004) Role of aryl hydrocarbon receptor-mediated induction of the CYP1 enzymes in environmental toxicity and cancer. *J Biol Chem* **279**: 23847-23850.

NIH-DCTD Aminoflavone Toxicology Summary. https://dctd.cancer.gov/featuredagents/pdfs/710464aminoflavonetoxabstract.pdf

Okey AB (2007) An aryl hydrocarbon receptor odyssey to the shores of toxicology: the Deichmann Lecture, International Congress of Toxicology-XI. *Toxicol Sci* **98**: 5-38.

Powell JB, Goode GD and Eltom SE (2013) The Aryl Hydrocarbon Receptor: A Target for Breast Cancer Therapy. *J Cancer Ther* **4**: 1177-1186.

Rexer BN, Engelman JA and Arteaga CL (2009) Overcoming resistance to tyrosine kinase inhibitors: lessons learned from cancer cells treated with EGFR antagonists. *Cell Cycle* **8**: 18-22.

Safe S and Wormke M (2003) Inhibitory aryl hydrocarbon receptor-estrogen receptor alpha cross-talk and mechanisms of action. *Chem Res Toxicol* **16**: 807-816.

Schlezinger JJ, Liu D, Farago M, Seldin DC, Belguise K, Sonenshein GE and Sherr DH (2006) A role for the aryl hydrocarbon receptor in mammary gland tumorigenesis. *Biol Chem* **387**: 1175-1187.

Sharma P (2016) Biology and Management of Patients With Triple-Negative Breast Cancer. *Oncologist* **21**: 1050-1062.

Steeg PS (2016) Targeting metastasis. *Nat Rev Cancer* **16**: 201-218.

Tarleton M, Gilbert J, Robertson MJ, McCluskey A and Sakoff JA (2011) Library synthesis and cytotoxicity of a family of 2-phenylacrylonitriles and discovery of an estrogen dependent breast cancer lead compound. *Medicinal Chemistry Communications* **2**: 31-37.

Tian J, Feng Y, Fu H, Xie HQ, Jiang JX and Zhao B (2015) The Aryl Hydrocarbon Receptor: A Key Bridging Molecule of External and Internal Chemical Signals. *Environ Sci Technol* **49**: 9518-9531.

Trapani V, Patel V, Leong CO, Ciolino HP, Yeh GC, Hose C, Trepel JB, Stevens MF, Sausville EA and Loaiza-Perez AI (2003) DNA damage and cell cycle arrest induced by 2-(4-amino-3-methylphenyl)-5-fluorobenzothiazole (5F 203, NSC 703786) is attenuated in aryl hydrocarbon receptor deficient MCF-7 cells. *Br J Cancer* **88**: 599-605.

Vinothini G and Nagini S (2010) Correlation of xenobiotic-metabolizing enzymes, oxidative stress and NF kappa B signaling with histological grade and menopausal status in patients with adenocarcinoma of the breast. *Clinica Chimica Acta* **411**: 368-374.

Waldman SA (2002) Does potency predict clinical efficacy? Illustration through an antihistamine model. *Ann Allergy Asthma Immunol* **89**: 7-11; quiz 11-12, 77.

Walsh AA, Szklarz GD and Scott EE (2013) Human cytochrome P450 1A1 structure and utility in understanding drug and xenobiotic metabolism. *J Biol Chem* **288**: 12932-12943.

Wormke M, Stoner M, Saville B and Safe S (2000) Crosstalk between estrogen receptor alpha and the aryl hydrocarbon receptor in breast cancer cells involves unidirectional activation of proteasomes. *FEBS Lett* **478**: 109-112.

Wormke M, Stoner M, Saville B, Walker K, Abdelrahim M, Burghardt R and Safe S (2003) The aryl hydrocarbon receptor mediates degradation of estrogen receptor alpha through activation of proteasomes. *Mol Cell Biol* **23**: 1843-1855.

Yurttas L, Tay F and Demirayak S (2015) Synthesis and antitumor activity evaluation of new 2-(4-aminophenyl)benzothiazole derivatives bearing different heterocyclic rings. *J Enzyme Inhib Med Chem* **30**: 458-465.

Zhang S, Lei P, Liu X, Li X, Walker K, Kotha L, Rowlands C and Safe S (2009) The aryl hydrocarbon receptor as a target for estrogen receptor-negative breast cancer chemotherapy. *Endocr Relat Cancer* **16**: 835-844.

Molecular Pharmacology Fast Forward. Published on December 21, 2017 as DOI: 10.1124/mol.117.109827
This article has not been copyedited and formatted. The final version may differ from this version.

Footnote

This study was supported by grants from the Calvary Mater Newcastle Hospital Granting Scheme, the Hunter Medical Research Institute, and Hunter Cancer Research Alliance, NSW Australia.

Figure Legends

Figure 1. Structure of (A) (*Z*)-2-(3,4-dichlorophenyl)-3-(1*H*-pyrrol-2-yl)acrylonitrile (**ANI-7**); (B) 5-amino-2-(4-amino-3-fluorophenyl)-6,8-difluoro-7-methyl-4*H*-1-benzopyran-4-one (aminoflavone, AhR agonist); (C) Tamoxifen (ER antagonist); (D) 4-Hydroxytamoxifen (ER antagonist); (E) Raloxifene (ER antagonist/AhR agonist); (F) Anastrozole (aromatase inhibitor); (G) (*Z*)-3-(3,5-dichlorophenyl)-2-pyridin-3-ylprop-2-enenitrile (Tyrphostin, RG14620, EGFR inhibitor).

Figure 2. Growth inhibition response (MTT assay) of ANI-7 in various breast (red) and non-breast (blue) derived cell lines after 72 h continuous exposure showing sensitive (solid line) and non-sensitive (dash line) cell populations. Each data point is the mean ± the standard error of the mean (SEM) from 4-5 replicates.

Figure 3. Cell cycle analysis (percentage distribution) of MCF10A (A,B) and MDA-MB-468 (C,D) cells treated with (B,D) or without (A,C) ANI-7 (2.5 µM) for 24 h. Analysis was replicated on three occasions with one representative set shown.

Figure 4. MDA-MB-468 cells were treated with ANI-7 (2.0 µM) for 0, 12 and 24 h, and examined for (A) checkpoint activation (CHK2, pCHK2) and (B) DNA damage (H2AXɣ) by Western blotting. The relative optical density normalised to actin content is also shown. Data was replicated on two separate

Molecular Pharmacology Fast Forward. Published on December 21, 2017 as DOI: 10.1124/mol.117.109827
This article has not been copyedited and formatted. The final version may differ from this version.

occasions, with one representative set shown. Data for (A) and (B) were from the same experiment and blots were performed on the same gel, therefore the same loading control was used for both panels.

Figure 5. Growth inhibition response (MTT assay) in MDA-MB-468 cells after 72 h of ANI-7 (0.1 μM) and aminoflavone (3 pM) in the presence and absence of (A) the AhR antagonist CH223191 (5 μM) and (B) the CYP1 inhibitor α-naphthoflavone (10 μM). Each data point is the mean ± SEM of three replicates. (C) Fold change in expression of AhR in MDA-MB-468 cells in the presence (AhR siRNA) or absence (scrambled siRNA) of AhR knockdown. (D) Growth inhibition response in MDA-MB-468 cells after 72 h of ANI-7 (1.0 μM) in the presence (AhR siRNA) or absence (scrambled siRNA) of AhR siRNA. Each data point is the mean ± SEM of two replicate experiments.

Figure 6. (A) Induction of XRE activity using a reporter assay in MDA-MB-468 cells after 6 h of ANI-7 (0.2 and 2 μM) treatment. Each data point is the mean ± SEM of two replicate experiments. (B-F) Change in gene expression (q PCR) in MDA-MB-468 cells of (B) AhR, (C) CYP1A1, (D) CYP1A2, (E) CYP1B1 and (F) SULT1A1 after 1-24 h treatment of ANI-7 (2 μM) compared with untreated control cells (Unt).

Figure 7. Inherent gene expression (qPCR) of (A) AhR, (B) ARNT, (C) CYP1A1, (D) CYP1A2, (E) CYP1B1, and (F) SULT1A1 in our panel of cell lines.

Molecular Pharmacology Fast Forward. Published on December 21, 2017 as DOI: 10.1124/mol.117.109827
This article has not been copyedited and formatted. The final version may differ from this version.

Table 1. Growth inhibition response (MTT assay, 72h) (GI_{50} values μM, concentration that inhibits growth by 50%) of ANI-7 and various breast cancer targeting agents in a broad panel of cancer cell lines. Data represents the mean ± SEM of 4-5 replicates.

Cell Line	ANI-7	Tamoxifen	Hydroxy tamoxifen	Raloxifene	Anastrozole	Tyrphostin RG14620	Amino flavone
MCF-7[a]	0.38 ± 0.03	7.7 ± 0.6	4.2 ± 1.2	8.7 ± 3.3	35 ± 16	12 ± 1	0.006±0.001
A431[b]	0.51 ± 0.05	6.5 ± 1.0	8.8 ± 0.4	14 ± 2	>50	12 ± 0.75	7.4 ± 0.7
H460[c]	3.0 ± 0.4	9.5 ± 0.3	2.5 ± 0.4	12 ± 0.8	>50	16 ± 0.4	0.16 ± 0.05
HT29[d]	6.0 ± 0.2	8.2 ± 1.9	2.0 ± 0.1	11 ± 2	>50	5.8 ± 1.5	21± 5
A2780[e]	13 ± 2	13 ± 1.2	7.1 ± 0.7	9.5 ± 0.4	>50	10 ± 1.0	0.32 ± 0.09
BE2-C[f]	18 ± 2	16 ± 0.3	2.8 ± 0.3	15 ± 0	>50	10 ± 0.67	21 ± 2
SMA[g]	20 ± 2	12 ± 0.3	7.9 ± 0.2	16 ± 2	>50	15 ± 2.0	14±1
SJ-G2[h]	23 ± 2	12 ± 2	8.6 ± 0.5	17 ± 0	>50	9.5 ± 1.3	12 ± 1
Du145[i]	27 ± 1	10 ± 3	8.9 ± 0.6	12 ± 0	>50	11 ± 0.43	12 ± 1
U87[h]	36 ± 3	18 ± 2	9.5 ± 0.6	21 ± 1	>50	13 ± 0.82	14 ± 1
SW480[d]	39 ± 3	16 ± 0.3	2.0 ± 0.1	nd[j]	>50	18 ± 0.86	nd
MIA[k]	42 ± 3	10 ± 0.3	6.0 ± 0.5	14 ± 2	>50	12 ± 0.0	13 ± 2

[a] breast carcinoma, [b] skin carcinoma, [c] lung carcinoma, [d] colon carcinoma, [e] ovary carcinoma, [f] neuroblastoma, [g] spontaneous murine astrocytoma, [h] glioblastoma, [i] prostate carcinoma, [j] not determined, [k] pancreatic carcinoma.

Molecular Pharmacology Fast Forward. Published on December 21, 2017 as DOI: 10.1124/mol.117.109827
This article has not been copyedited and formatted. The final version may differ from this version.

Table 2. Growth inhibition response (MTT assay, 72h) (GI_{50} values μM, concentration that inhibits growth by 50%) of ANI-7 and various breast cancer targeting agents in a panel of breast cancer cell lines. Data represents the mean ± SEM of 4-5 replicates.

Cell Line	ANI-7	Tamoxifen	Hydroxy tamoxifen	Raloxifene	Anastrozole	Tyrphostin RG14620	Amino flavone
T47D[a]	0.16 ± 0.02	4.7 ± 0.3	3.1 ± 0.4	7.2 ± 0.5	26 ± 0	9.6 ± 0.6	0.04 ± 0.02
ZR-75-1[a]	0.18 ± 0.02	5.8 ± 0.3	4.8 ± 1.2	7.2 ± 1.2	22 ± 14	14 ± 2	0.002 ± 0.02
MCF-7/VP16[a]	0.21 ± 0.4	nd[b]	nd	nd	33 ± 17	11 ± 0.0	nd
MCF-7[a]	0.38 ± 0.03	7.7 ± 0.6	4.2 ± 1.2	8.7 ± 3.3	35 ± 16	13 ± 1.3	0.02 ± 0.0
SKBR3[c]	0.21 ± 0.03	7.1 ± 0.2	7.2 ± 0.1	7.3 ± 0.9	nd	8.5 ± 0.5	0.005 ± 0.03
MDA-MB-468[d]	0.23 ± 0.01	8.0 ± 0.0	8.2 ± 0.3	14 ± 0.7	nd	8.8 ± 0.2	0.001 ± 0.01
BT474[a]	1 ± 0.3	7.4 ± 0.4	7.4 ± 1.0	9.0 ± 2.1	nd	10 ± 1	0.8 ± 0.3
BT20[d]	2 ± 0.4	8.5 ± 0.0	9.0 ± 0.0	16 ± 0.8	nd	13 ± 0.7	7.0 ± 1.5
MDA-MB-231[d]	17 ± 4	9.0 ± 0.03	12 ± 0.3	20 ± 0.6	33 ± 18	17 ± 1	20 ± 0.7
MCF10A[e]	26 ± 3	9.7 ± 0.6	11 ± 0.3	16 ± 0.3	>50	11 ± 1	16 ± 0.3

[a] ER(Estrogen receptor) positive, [b] not determined, [c] ER negative HER2 positive, [d] triple negative for ER, PR and HER2, [e] normal breast cell line.

Molecular Pharmacology Fast Forward. Published on December 21, 2017 as DOI: 10.1124/mol.117.109827
This article has not been copyedited and formatted. The final version may differ from this version.

Table 3. *In vitro* ER and aromatase inhibition (IC_{50} μM) assay in the presence of ANI-7, Tamoxifen, hydroxy tamoxifen and anastrozole. Data represents the mean ± SEM of three replicate experiemnts.

	ER Inhibition (IC_{50} μM)	Aromatase Inhibition (IC_{50} μM)
ANI-7	> 2	>100
Tamoxifen	0.012 ± 0.009	nd[a]
4-Hydroxy Tamoxifen	0.0017 ± 0.0007	nd
Anastrazole	nd	0.12 ± 0.07

[a] not determined

Molecular Pharmacology Fast Forward. Published on December 21, 2017 as DOI: 10.1124/mol.117.109827
This article has not been copyedited and formatted. The final version may differ from this version.

Table 4. Percentage kinase activity in the presence of 10 μM ANI-7. The data represent the mean ± SEM of duplicate experiments

Receptors		
EGFR	101 ± 1	[a]
ERBB2/HER2	95 ± 3	[a]
ERBB4/HER4	102 ± 6	[a]
IGF1R	90 ± 7.2	[b]
PDGFRa	87 ± 8.5	[a]
PDGFRb	102 ± 2.3	[a]
Lipid Kinases		
Choline Kinase Alpha	97 ± 2.4	[b]
Choline Kinase beta	97 ± 4.1	[b]
DGK beta	93 ± 30	[b]
DGK gamma	83 ± 20	[b]
DGK zeta	88 ± 14	[b]
PI3 kinase alpha	84 ± 1.9	[a]
PI3 kinase beta	95 ± 6.9	[a]
PI3 kinase delta	77 ± 8.3	[a]
PI3 kinase gamma	66 ± 12	[a]
PI4K2A	94 ± 8.4	[b]
PIP5K2A	83 ± 0.6	[b]
Sphingosine kinase 1	65 ± 23	[b]
Sphingosine kinase 2	80 ± 8.9	[b]
Others		
BRK	91 ± 4.6	[a]
PKBa	101 ± 0.2	[b]
PKD1	119 ± 0.1	[b]
PKBb	99 ± 9.0	[b]

PI3K/mTOR pathway		
PDK1/PDPK1	95 ± 1.4	[a]
SGK1	95 ± 0.8	[a]
SGK2	93 ± 1.1	[a]
SGK3/SGKL	99 ± 3.1	[a]
AKT1	94 ± 2.3	[a]
AKT2	91 ± 1.9	[a]
AKT3	104 ± 2.0	[a]
COT1/MAP3K8	95 ± 0.8	[a]
GSK3a	80 ± 0.3	[a]
GSK3b	89 ± 1.5	[a]
mTOR/FRAP1	98 ± 0.7	[a]
ROCK1	95 ± 2.3	[a]
ROCK2	98 ± 0.3	[a]
P70S6K	103 ± 3.0	[b]
MAP Kinase pathway		
RAF1	106 ± 1.3	[a]
ARAF	100 ± 2.3	[a]
BRAF	101 ± 1.2	[a]
MEK1	101 ± 1.5	[a]
MEK2	92 ± 0.3	[a]
ERK1	100 ± 1.6	[a]
ERK2/MAPK1	98 ± 0.7	[a]
c-Src	87 ± 4.6	[a]

[a] Reaction Biology Corporation USA, [b] The International Centre for Kinase Profiling University of Dundee UK.

Molecular Pharmacology Fast Forward. Published on December 21, 2017 as DOI: 10.1124/mol.117.109827
This article has not been copyedited and formatted. The final version may differ from this version.

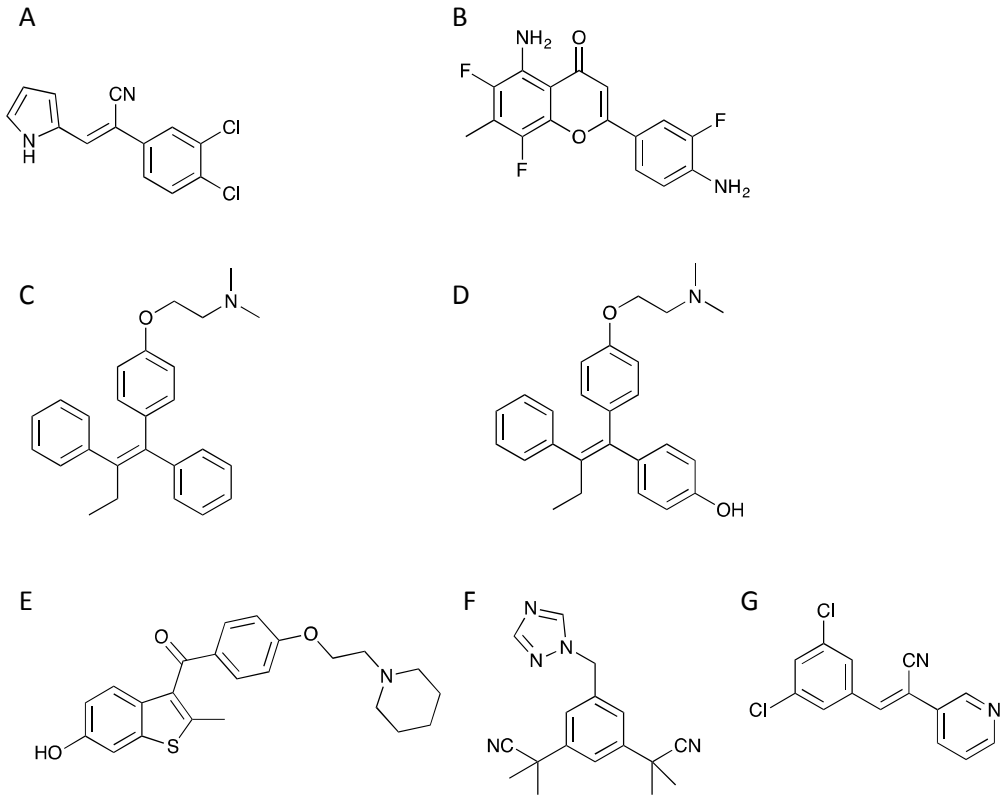

Figure 1.

Molecular Pharmacology Fast Forward. Published on December 21, 2017 as DOI: 10.1124/mol.117.109827
This article has not been copyedited and formatted. The final version may differ from this version.

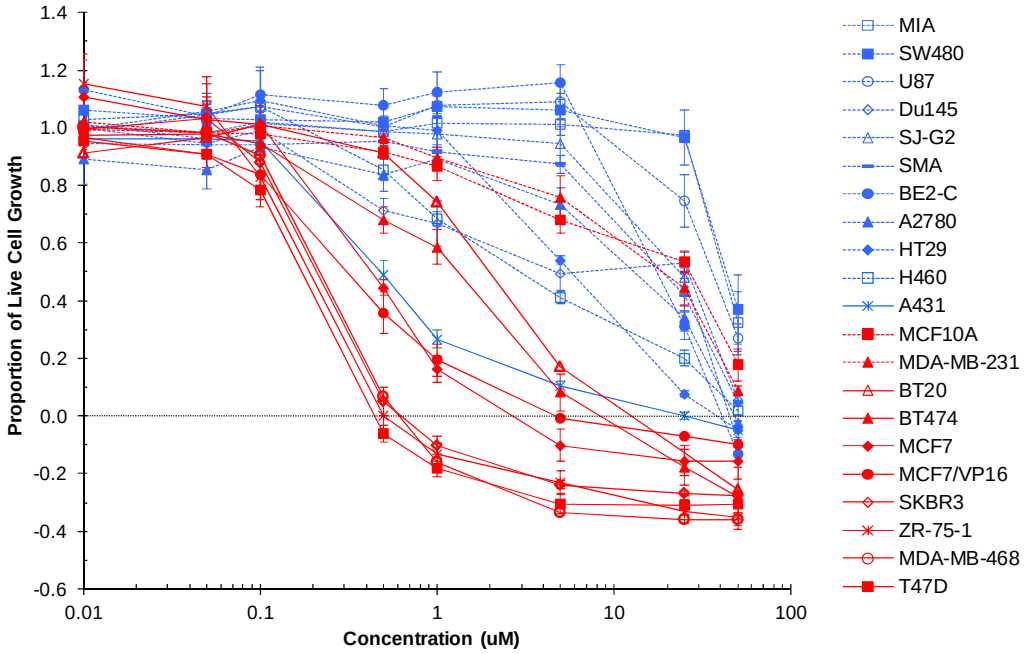

Figure 2.

Molecular Pharmacology Fast Forward. Published on December 21, 2017 as DOI: 10.1124/mol.117.109827
This article has not been copyedited and formatted. The final version may differ from this version.

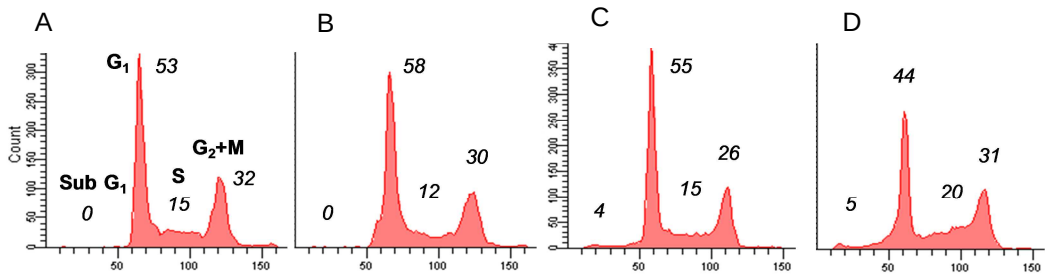

Figure 3.

Molecular Pharmacology Fast Forward. Published on December 21, 2017 as DOI: 10.1124/mol.117.109827
This article has not been copyedited and formatted. The final version may differ from this version.

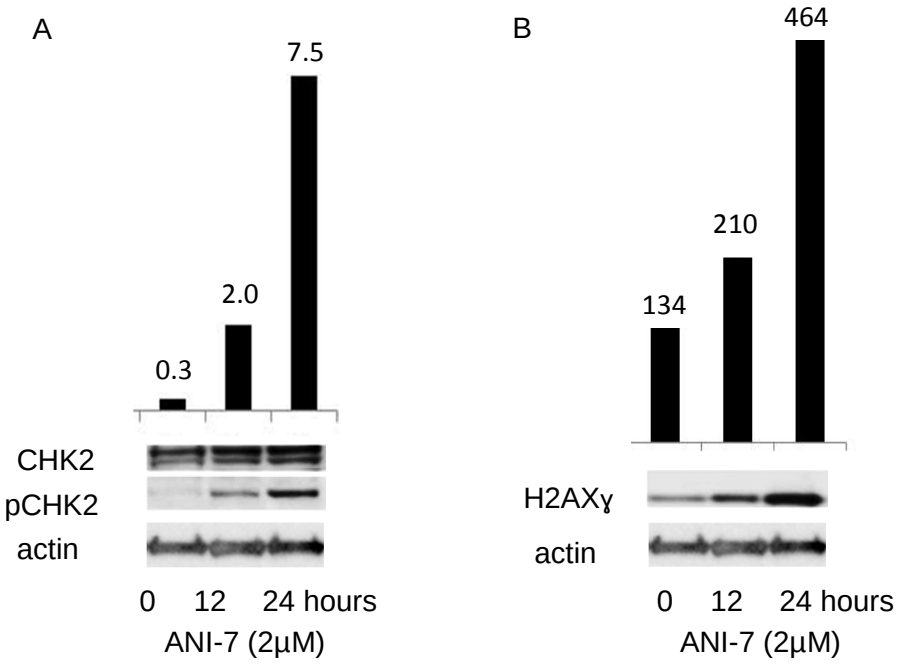

Figure 4.

Molecular Pharmacology Fast Forward. Published on December 21, 2017 as DOI: 10.1124/mol.117.109827
This article has not been copyedited and formatted. The final version may differ from this version.

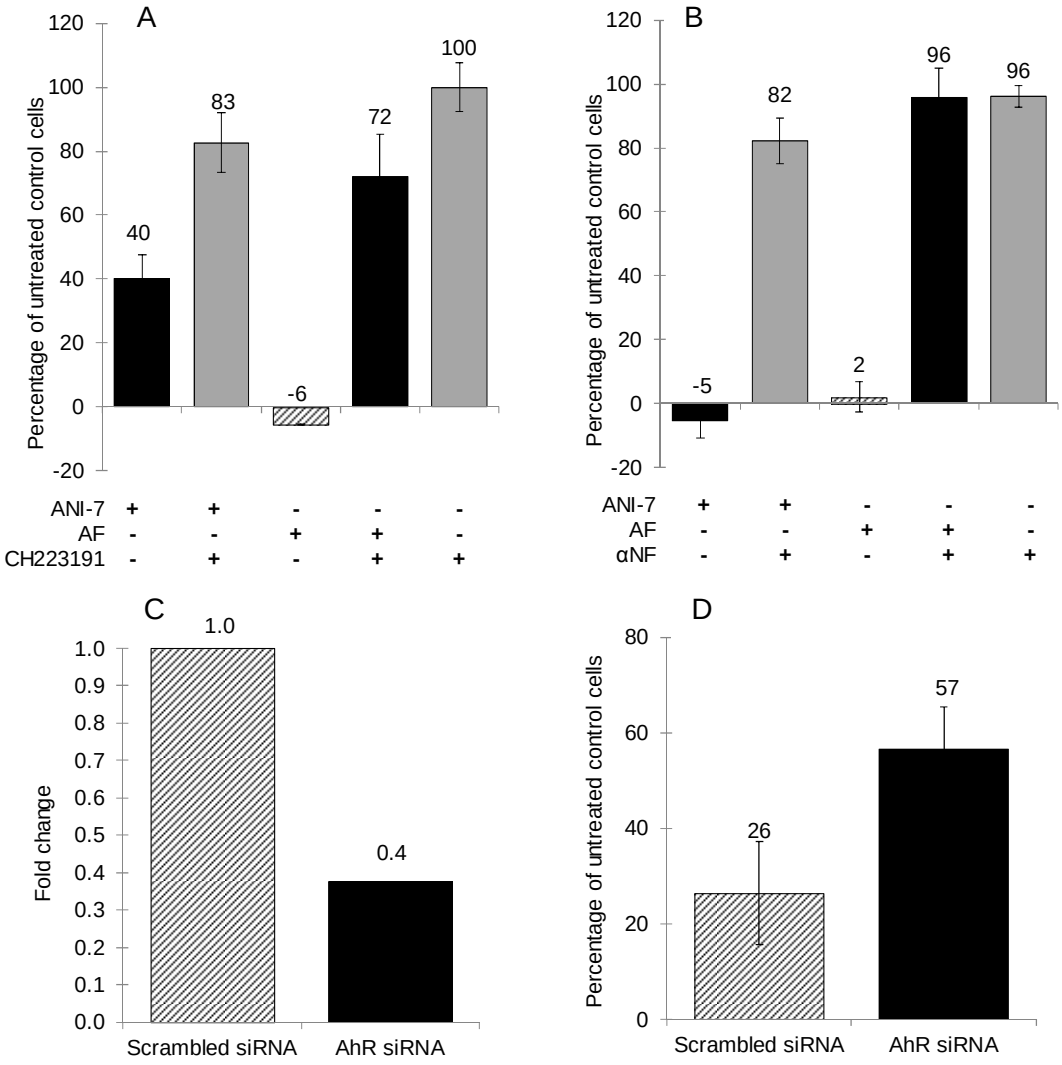

Figure 5.

Molecular Pharmacology Fast Forward. Published on December 21, 2017 as DOI: 10.1124/mol.117.109827
This article has not been copyedited and formatted. The final version may differ from this version.

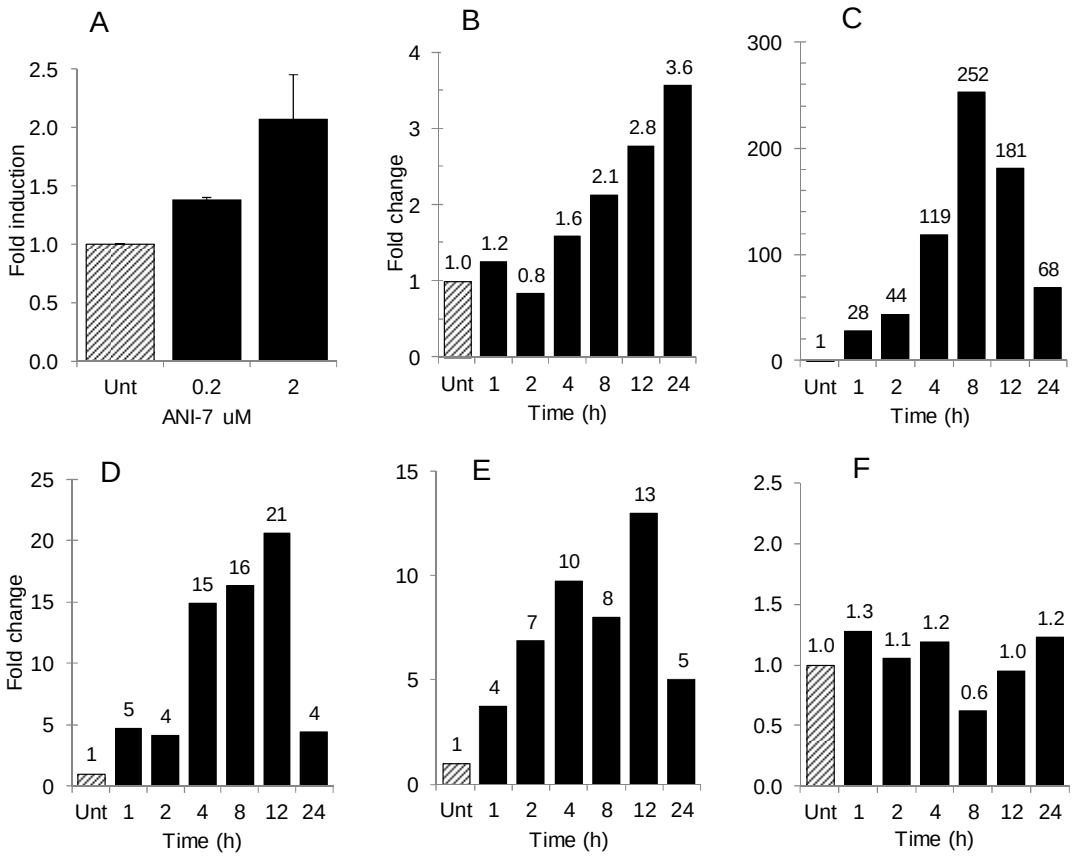

Figure 6.

Molecular Pharmacology Fast Forward. Published on December 21, 2017 as DOI: 10.1124/mol.117.109827
This article has not been copyedited and formatted. The final version may differ from this version.

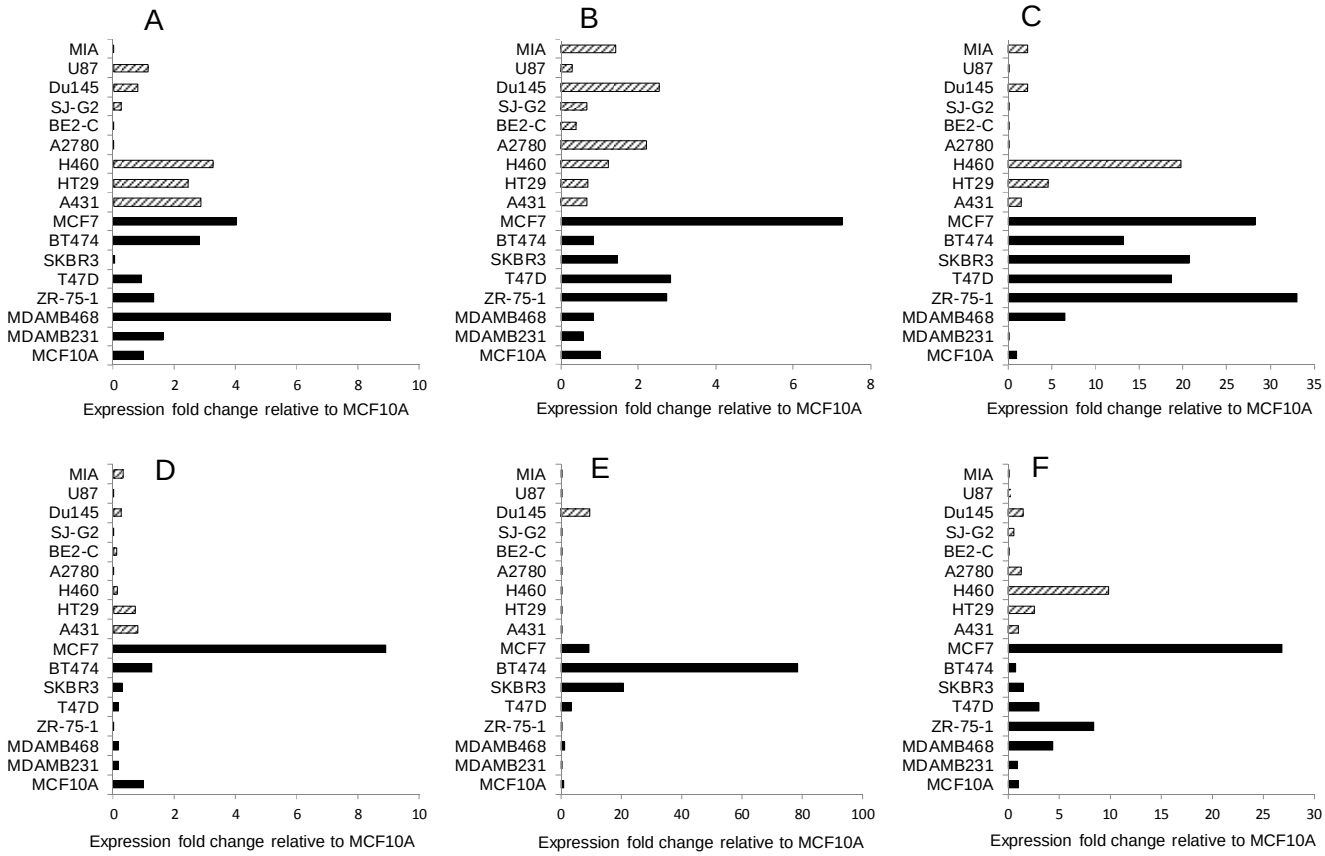

Figure 7.